

A MODULAR APPROACH TO INTEGRATED ENERGY DISTRIBUTION SYSTEM ANALYSIS

Marc Rees Cardiff University ReesMT@cf.ac.uk	Jianzhong Wu Cardiff University WuJ5@cf.ac.uk	Bieshoy Awad Cardiff University AwadBA@cf.ac.uk	Janaka Ekanayake Cardiff University EkanayakeJ@cf.ac.uk	Nick Jenkins Cardiff University JenkinsN6@cf.ac.uk
---	--	--	--	---

Abstract – An integrated steady state heat and power distribution analysis tool was developed. The distribution system was represented as a set of interacting network and generation plant modules. System operation was determined on a minimum cost basis at each time step. The model was used to compare the performance of two community generation options integrating biomass with natural gas CHP for a case study based on a proposed new build development in the UK.

Keywords: *Integrated heat and electricity analysis, Combined Heat and Power, Biomass, modular modeling, low carbon infrastructure.*

1 INTRODUCTION

The integration of electricity and heat generation with district heating and electricity distribution networks can potentially provide significant carbon savings compared to the use of individual gas boilers with imported electricity[1-5]. The impacts and benefits of system integration have been explored by a number of authors [6-8] but are often not adequately incorporated into design and feasibility studies of real systems. This may lead to financially viable low carbon design options being overlooked through inadequate analysis and poorly informed best practice.

The combined analysis of heat and power systems has received attention in a number of studies as in [9-12]. The most common approach is to treat the heat and power networks as a set of flow or capacity constraints. A novel approach developed by Geidl[12] considers the system as a set of connected energy hubs collectively represented by an energy conversion matrix.

This paper presents a modular approach to combined steady state energy distribution analysis for use within detailed financial appraisal and project life emissions evaluation. A case study was used to demonstrate application of the model to the study of two potential supply options for a proposed new build community re-development in the UK.

2 COMPONENT MODULARISATION

The heat and power distribution system was divided into a set of modules each representing a specific aspect of the infrastructure. The integrated infrastructure was then modelled as a set of interacting modules. This ap-

proach allows the use of well established network load flow techniques and generation plant models without any loss of integrity. The network spacial information and generation plant design detail are therefore retained within the analysis.

2.1 General form

Each network and generation plant module was constructed using a set of fixed known parameters (plant specifications, network topology etc.) combined with an appropriate steady state analysis method (Fig. 1).

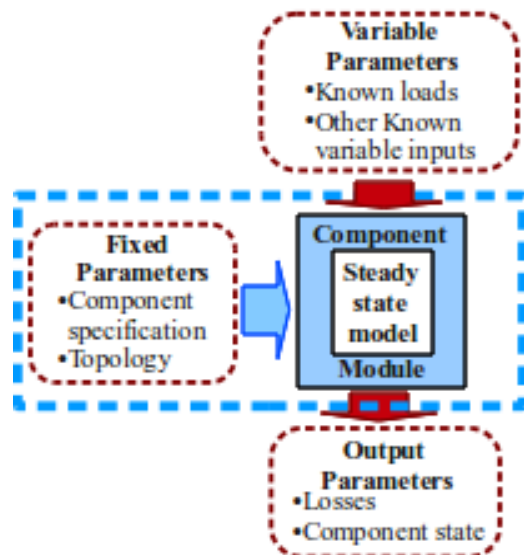


Figure 1: Generic form of steady state analysis module.

2.2 Generation plant module

The module representing plant j was initially constructed by specifying plant type, rated heat production, minimum plant downtime $\zeta_{min}^{(j)}$, rated electrical generation efficiency $\eta_{th,rated}^{(j)}$ and fuel conversion efficiency $\eta_{Fcon}^{(j)}$. Other parameters such as working fluid temperature and part load performance were stored as within the module as functions of plant type and rated capacity.

The plant heat generation $\phi^{(j)}$ was used as the module method input variable and corresponds to the total quantity of heat produced by the plant before recovery to the district heat network (DHN). This allows a consistent modeling approach for heat only, power only and CHP units and removes dependence on the type of heat application use. The module output variables were the electrical power generated P_G and plant fuel con-

sumption F . The steady state analysis method depends upon the plant type:

2.2.1 Heat only boilers.

For natural gas and biomass heat only boilers, $P_G^{(j)}=0$. The fuel energy input at time step p is given by:

$$F^{(j,p)} = \Phi_G^{(j,p)} / \eta_{Fcon}^{(j)} \quad (1)$$

2.2.2 Internal combustion engines (ICE's).

The power output was defined in terms of $\Phi^{(j)}$:

$$P_G^{(j)} = \frac{\eta_{th}}{(1-\eta_{th})} \Phi^{(j)} \quad (2)$$

Electrical efficiency η_{th} is a function of part load fraction $\zeta^{(j)} \Phi_{max}^{(j)}$ and $\eta_{th,rated}^{(j)}$. The plant fuel energy input was:

$$\Phi_{fuel}^{(j)} = (P_G^{(j)} + \Phi^{(j)}) / \eta_{comb}^{(j)} \quad (3)$$

2.3 Power distribution network module

The power distribution network module was constructed by defining the network topology and line specification data. It was used to determine network losses, imported power, maximum network voltage, minimum network voltage and maximum current. Analysis inputs were local power generation P_G and demand P_D . The analysis method used a forward / backward radial load flow. A flow diagram for the analysis algorithm is shown in Fig. 2.

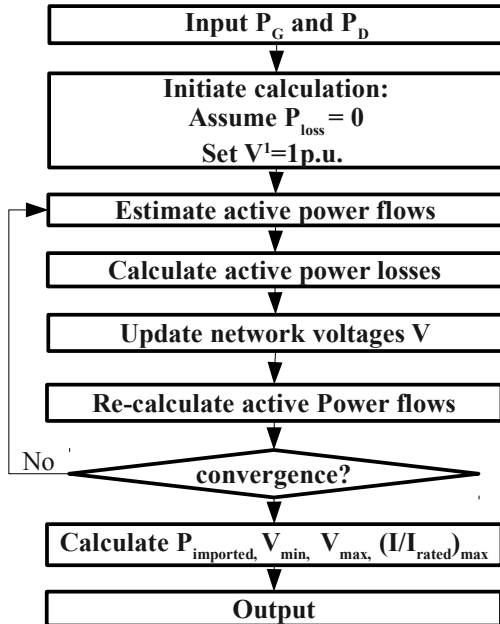


Figure 2: Flow diagram for power network module.

2.4 District heat network module

The district heating module was constructed by defining the network topology, pipe specification data and design supply and return temperature data. It was used to determine network heat losses $\Phi_{loss}^{(p)}$ and the maximum network flow velocity. The module inputs were the

heat recovered from the generation unit to the heat network $\Phi_G^{(p)}$ and the consumer cluster demand $\Phi_C^{(p)}$. The steady state analysis algorithm is illustrated by Fig. 3. The vector of consumer flow rates $f_C^{(p)}$ was initially estimated using

$$\Phi_C^{(p)} = c_p (f_C^{(p)})^T (T_s - T_r) \quad (4)$$

There T_s and T_r are the supply and return temperatures and c_p the specific heat capacity. The heat supply ratio between plants was assumed constant within the analysis so that $\Phi_G^{(p)} = (\sum \Phi_D^{(p)} + \Phi_{loss}^{(p)}) x_G^{(p)}$, where x_G is the fraction supply vector calculated by initially ignoring network losses. The generation plant flows $f_G^{(p)}$ were calculated from

$$(\sum \Phi_D^{(p)} + \Phi_{loss}^{(p)}) x_G^{(p)} = c_p (f_G^{(p)})^T (T_s - T_r) \quad (5)$$

The vector of pipe mass flow rates \dot{m} was then obtained from

$$A \dot{m}^{(p)} = f^{(p)} = f_G^{(p)} - f_C^{(p)} \quad (6)$$

where A is the network incidence matrix. The pipe temperature loss, pipe node flow balance and perfect mixing assumption at each node were represented using

$$T_{out} = T_{in} e^{-\frac{(U \pi d l)}{(4 \dot{m})}} \quad (7)$$

$$\sum \dot{m}_{in} - \sum \dot{m}_{out} = 0 \quad (8)$$

$$T_{out} \sum \dot{m} - \sum T_{in} \dot{m} = 0 \quad (9)$$

which are combined to solve for T , the vector of node temperatures. The new temperatures were then used to re-estimate consumer and supply flows. The calculation was repeated until mass flow rate convergence.

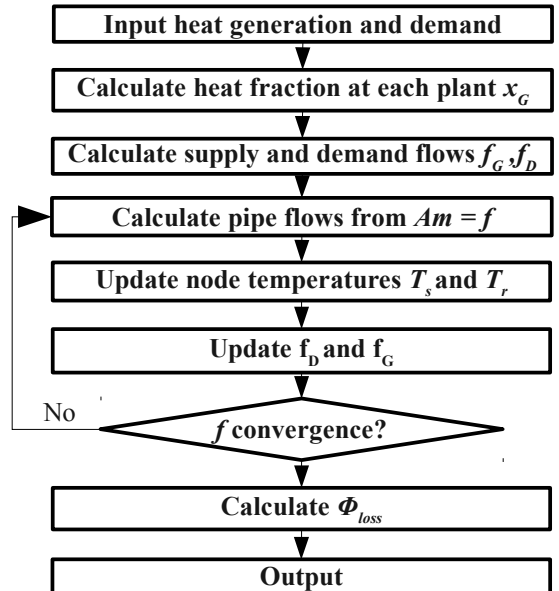


Figure 3: Flow diagram of DHN module

3 MODULE INTERACTION

A computational architecture was developed to run the integrated system analysis as a set of interacting modules. This determined the operational cost and system emissions at each time step. A non linear optimisation

solver was used to apply the minimum cost operation assumption and system constraints.

3.1 Decision variables

The plant waste heat output $\Phi^{(j)}$ and the plant on/off status $\delta_G^{(j,p)}$ were used as the analysis decision variables at each time step.

3.1.1 Generation plant heat output

The solver algorithm assigned a dummy value to waste heat production $\Phi^{*(j,p)}$ for each generation plant at time-step p . Values were constrained between the minimum and maximum allowable outputs:

$$\Phi_{rated}^{(j)} - \Phi^{*(j)} \geq 0 \quad (10)$$

and

$$\Phi^{*(j)} - \Phi_{min}^{(j)} \geq 0 \quad (11)$$

The heat output available to the DHN was therefore

$$\Phi_G^{*(j,p)} = K_{DH} \Phi^{*(j,p)} \quad (12)$$

where K_{DH} is the heat exchanger recovery factor.

3.1.2 Generation plant index and on/off variable

Each plant type was assigned a binary heat recovery index $\delta_{heat}^{(j)}$ so that $\delta_{heat}^{(j)} = 1$ for CHP and heat generation units, and $\delta_{heat}^{(j)} = 0$ for power only generation plant. The heat recovered to the DHN was thus given by

$$\Phi_G^{(j,p)} = \delta_{heat}^{(j)} \delta_G^{(j,p)} \Phi_G^{*(j,p)} \quad (13)$$

The corresponding power output $P^{*(j,p)}$ was then calculated for each plant. The actual power output to the power distribution network was therefore:

$$P_G^{(j,p)} = \delta_G^{(j,p)} P^{*(j,p)} \quad (14)$$

3.2 System Constraints

System constraints were used by the solver to define the interaction behaviour of between modules:

3.2.1 Power network power balance constraint

The electrical power balance at each time step was defined using:

$$\sum_1^j P_G^{(j,p)} - \sum_1^i P_D^{(i,p)} - P_{losses}^{(p)} + P_{import}^{(p)} = 0 \quad (15)$$

For island modes of operation $P_{import}^{(p)} = 0$. $P_{import}^{(p)}$ and $P_{loss}^{(p)}$ were determined using the power distribution module.

3.2.2 Power network operational constraints

Adherence to statutory operational limits was enforced by applying the following set of constraints:

$$V_{max} \geq V_{upper} \quad (16)$$

$$V_{lower} \geq V_{min}^{(p)} \quad (17)$$

$$(I/I_{rated})_{max}^{(p)} \leq 1 \quad (18)$$

3.2.3 DHN balance constraint

The DHN was assumed to be a hydro-statically isolated system so that:

$$\sum_1^j \Phi_G^{(j,p)} - \sum_1^i \Phi_D^{(i,p)} - \Phi_{losses}^{(p)} = 0 \quad (19)$$

The heat network losses $\Phi_{losses}^{(p)}$ were determined using the heat network module.

3.3 Cost function

The solver was used to determine the set of $\Phi^{(j)}$ corresponding to minimum operational cost at each time step over the project time horizon. The annual cost of operation of plant j is:

$$c^{(j)} = \sum c_{opex}^{(j)} + \sum (c_{fuel}^{(j)} + c_{CCL}^{(j)}) \cdot F_G^{(j,p)} - \sum c_{PSales}^{(j)} + (c_{RO} + c_{LEC}) \cdot P_{QPO}^{(j)} - c_{RHI}^{(j)} \quad (20)$$

with the total annual cost defined as

$$C_{total} = \sum c^{(j)} - c_{\Phi sales} \quad (21)$$

3.3.1 Operational Expenditure

The operational expenditure C_{opex} was calculated on an annualised basis as a function of the plants rated capacity. At each time step therefore

$$c_{opex} = \frac{\tau^{(p)} C_{opex}^{(j)} \Phi_{rated}^{(j)}}{8760} \quad (22)$$

Where $C_{opex}^{(j)}$ is the operational expenditure per unit rated output (£/kW/year).

3.3.2 Heat revenue

The heat sales revenue was calculated assuming a constant tariff for all consumers so that

$$c_{\Phi sales} = c_{WSHeat} \sum \Phi_D^{(i,p)} \quad (23)$$

The renewable heat incentive (RHI) rewards renewable heat generation on the basis of plant output.

$$c_{RHI}^{(j)} = c_{RHItariff} \sum \Phi_G^{(j)} \quad (24)$$

3.3.3 Power revenue

It was assumed that the power generated by each production plant was sold to a supplier at the electricity wholesale price. The sales revenue was therefore:

$$c_{PSales}^{(j)} = \sum c_{WSpow} P_G^{(j)} \quad (25)$$

Renewable CHP plant qualify for renewable obligation certificates (ROC's) by accreditation through the CHPQA scheme[13]. This measures the quality of a CHP plant on the basis of its electrical efficiency and an overall quality index (QI). The first requirement is that new CHP plant must obtain $\eta_{el} \geq \eta_{thresh}$, where η_{thresh} is the minimum power generation efficiency defined within the standard. Failure to meet this threshold reduces the qualifying fuel input F_{QFI} such that:

$$F_{QFI}^{(j)} = F_{TFI}^{(j)} \frac{\eta_{el}}{\eta_{thresh}} \quad (26)$$

The QI is a weighted measure of the plant heat and power efficiencies defined as

$$QI^{(j)} = X^{(j)} \eta_{el} + Y^{(j)} \eta_{heat} \quad (27)$$

where X and Y are defined within CHPQA guidance in terms of plant type and size. The QI index was used to determine the qualifying power output P_{QPO} eligible for renewable energy subsidies and levy exception. If

$QI^{(j)} \geq QI_{thresh}$, $P_{QPO}^{(j)} = \sum P_G^{(j)}$. If $QI^{(j)} < QI_{thresh}$, calculation of P_{QPO} is dependent upon the type of plant. For non steam turbine units, the calculation of P_{QPO} is

$$P_{QPO}^{(j)} = \frac{Y^{(j)} \eta_{power}^{(j)} \Phi_{QHO}^{(j)}}{100 - X^{(j)} \eta_{power}^{(j)}} \quad (28)$$

where $\Phi_{QHO}^{(j)}$ is the qualifying heat output and $\eta_{power}^{(j)}$ is the annual plant electrical efficiency.

3.4 Non-linear optimisation solver

The lack of gradient information from each module prescribed the use of a direct search or meta-heuristic optimisation method. A hybrid differential evolution particle swarm (DEPS) non linear optimisation solver was used to run the analysis at each time step and determine $\Phi^{(p)}$ corresponding to minimum cost. A full description including Java source code can be found at [14].

3.5 Unit commitment selection (on/off) algorithm.

A flow chart illustrating the unit commitment selection algorithm is shown in Fig. 4. At each time step, the plant configuration was represented as a bit pattern B of length J , with bit 1 corresponding to $\delta_G^{(p,1)}$ at plant 1 and so on. Each unit commitment combination is analysed in turn starting from $B=0\dots01_2$ and increasing as a binary numeral by 1 until $B = (2^J-1)_{10}$. A feasibility algorithm was applied to identify infeasible plant combinations. The following tests were applied:

Test 1: if $\sum \Phi_{rated} < \Phi_{demand}$; not enough capacity within dispatch combination to meet demand.

Test 2: if $\sum \Phi_{min} < \Phi_{demand}$; Plant downtime constraints do not permit supply at the required level.

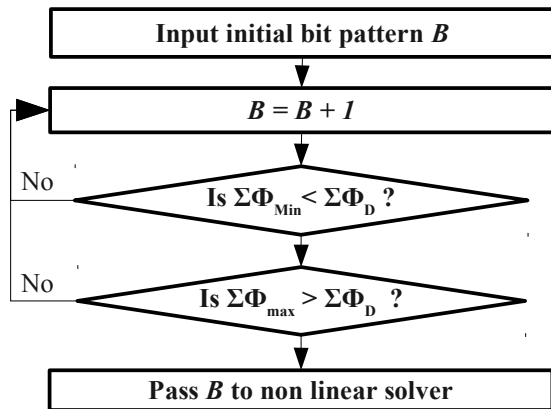


Figure 4: Flow diagram for Unit commitment search algorithm.

For systems with large numbers of generation units and time steps, it may be appropriate to consider additional efficiency measures including the use of dynamic programming to avoid analysis duplication over the time horizon. The complete structure of the integrated analysis environment is illustrated by Fig. 5.

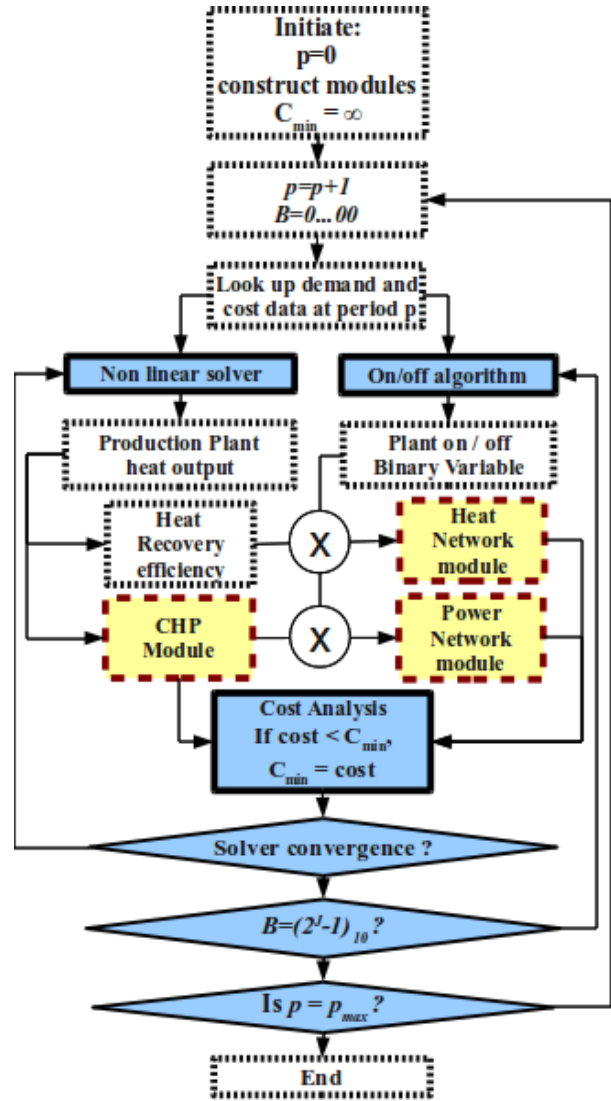


Figure 5: Flow diagram for the integrated modelling environment

4 IMPLEMENTATION AND CASE STUDY

The integrated modelling environment was implemented as an OpenOffice Calc spreadsheet. The steady state analysis modules were implemented as a set of Java classes using NetBeans and converted for implementation as Calc add in functions. A DEPS solver was used to perform the optimised plant output analysis. The candidate search algorithm was written as an Open Office Basic macro.

4.1 Case study description

An hypothetical case study was considered based upon a proposed new build private wire development in the UK. The model was applied to compare the performance of two alternative supply options integrating Biomass boilers with natural gas ICE CHP with the intention of reducing carbon emissions against a base level of 11,435tCO₂e for individual gas boilers with imported electrical power. Preliminary studies based on the an-

nual load duration curve (Fig. 6 and Fig. 7) indicated a significant carbon saving by trading CHP capacity with boiler capacity and a lower expected return on investment. The plant specification and estimated performance of each option is summarised in Table 1.

case	Community configuration
Option 1	Plant 1: 1040kWe NG ICE CHP Plant 2: 1840kWe NG ICE CHP Plant 3: 4000kWh Biomass boiler Plant 4: 10770kWh NG boilers.
Emissions < 9000tCO ₂ e/year, total plant capex = £5.21m expected IRR = 14%	
Option 2	Plant 1: 1070kWe NG ICE CHP Plant 2: 1200kWe NG ICE CHP Plant 3: 7000kWh Biomass boiler Plant 4: 10770kWh NG boilers.
Emissions < 8000tCO ₂ e/year, total plant capex = £5.47m expected IRR = 12%	

Table 1: Plant specifications for the two district heating supply options.

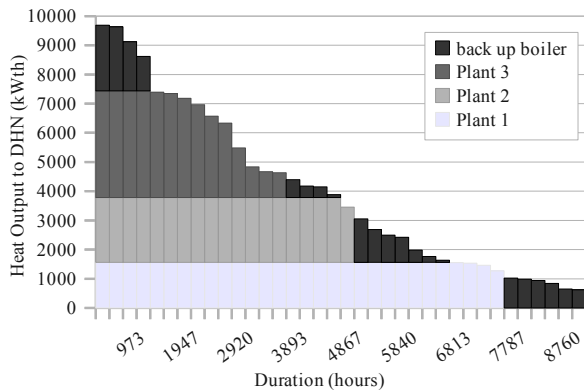


Figure 6: Estimated annual supply-duration curve (option 1).

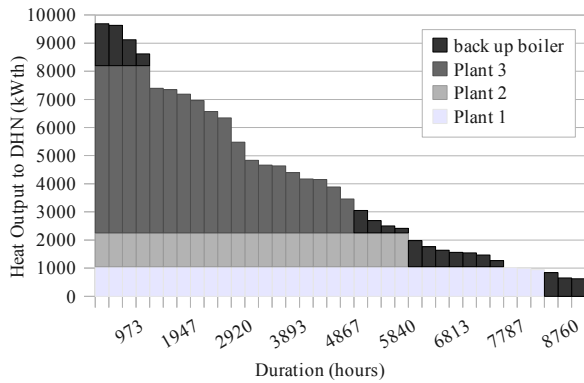


Figure 7: Estimated annual supply-duration curve (option 2).

The consumers were grouped into geographical clusters as defined within Table 2. The annual load profile for each was divided into a set of representative days each sub divided into 8 hour periods (Fig. 8 to Fig. 11).

Cluster No.	type	Peak DH demand (kW _{th})	DHN node	Peak power demand (kW _{th})	Power network location
1	Public buildings	4353	3	392	1
2	Residential	2416	5	698	2
3	mixed	2498	6	1084	3

Table 2: Consumer cluster data for case study development.

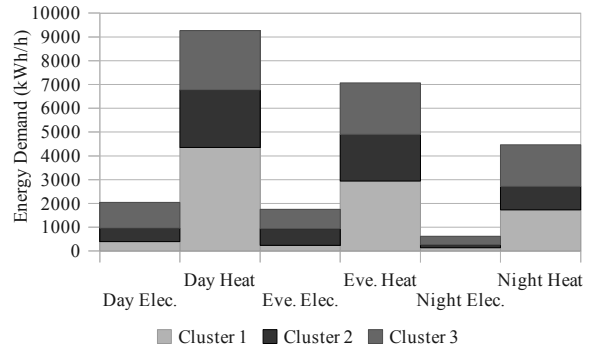


Figure 8: Representative day for Jan, Feb, March and Dec.

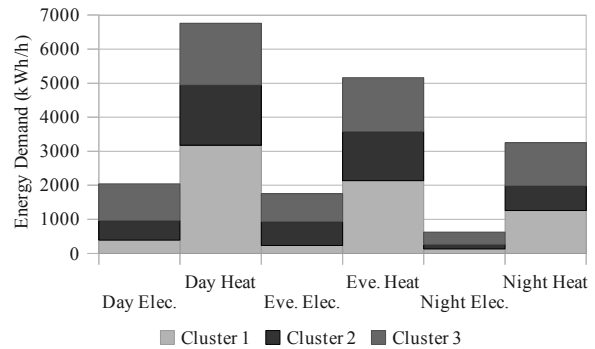


Figure 9: Representative day profile for April and Nov.

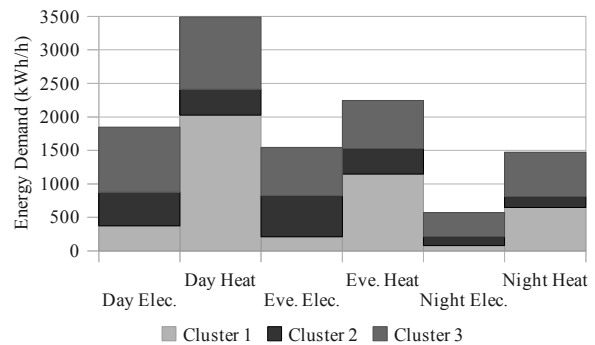


Figure 10: Representative day profile for May, Sept and Oct.

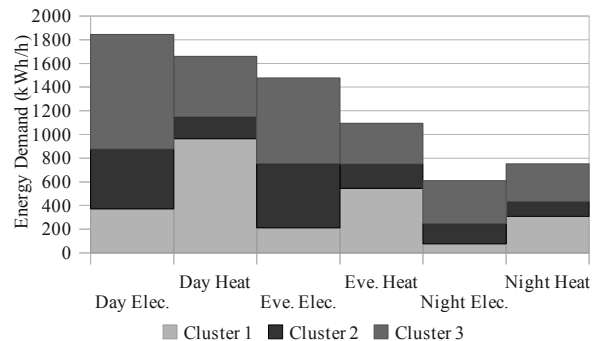


Figure 11: Representative day profile for June, July and Aug.

Construction specifications for the local DHN and 11kV distribution power network modules are shown in tables 3 and 4. Line 1 represents the primary 33/11kV

substation at the site boundary. Bus 0 was defined as the slack bus for load flow analysis.

Pipe	From node	To node	Length (m)	Diameter (mm)	U (W/m ² /K)
1	1	2	300	200	0.29
2	2	3	100	100	0.13
3	2	4	600	200	0.29
4	4	5	100	100	0.13
5	5	6	600	100	0.13

Table 3: Case study DHN module construction data. Supply temperature = 95°C, return temperature = 55°C.

line	From bus	To bus	Length (m)	X (Ω)	R (Ω)
0	0	1	200	0.038	0.016
1	1	2	600	0.114	0.048
2	2	3	600	0.114	0.048

Table 4: 11kV Power distribution network construction data

4.2 Case study results.

The annual supply duration curves for both options using the integrated analysis tool are shown within Fig. 12. When operating on a minimised cost basis natural gas CHP is prioritised where capacity constraints permit. Natural gas boilers are restricted to supply peak load only.

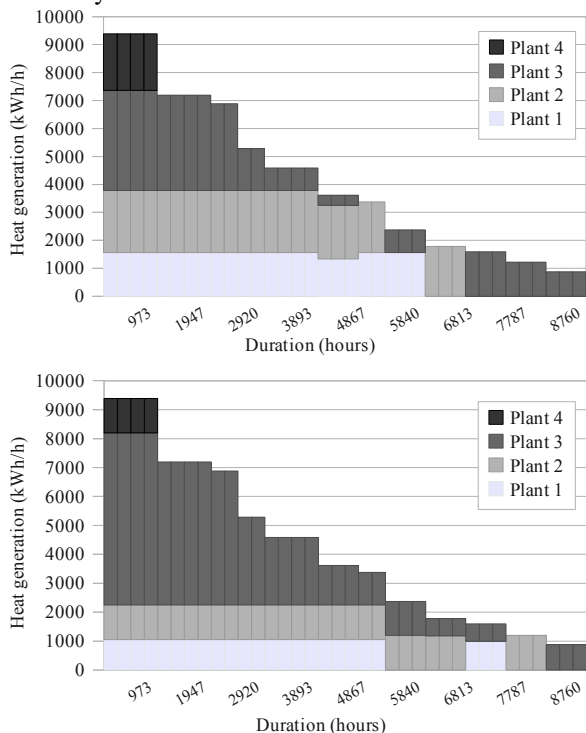


Figure 12: Supply-duration curves after integrated steady state analysis (Top = option 1, bottom = option 2).

The key results from the integrated analysis of the two systems is given by Table 5. The IRR for the generation plant has increased from the initial estimate by approximately 3%, which is attributable to the increased power generation revenue from CHP units and the additional RHI revenue from biomass units.

case	IRR	Greenhouse gas emissions (tCO ₂ e/year)
Option 1	17.30%	7840 (68% of base)
Option 2	15.59%	7630 (66% of base)

Table 5: Plant specifications for the two district heating supply options.

Optimising on a minimum cost basis decreases the annual site emissions of both options compared to the initial estimate. It is interesting to observe, however, that the difference between total annual emissions of each option is reduced to less than 3%. Fig. 13 shows the annual GHG emissions for both options using the same period sequence used within the supply-duration curve. Option 2 displays lower emissions at peak load conditions due to the larger specified biomass unit. At lower loads, biomass boilers are prescribed for option 1 due to the downturn constraints of the larger NG CHP units.

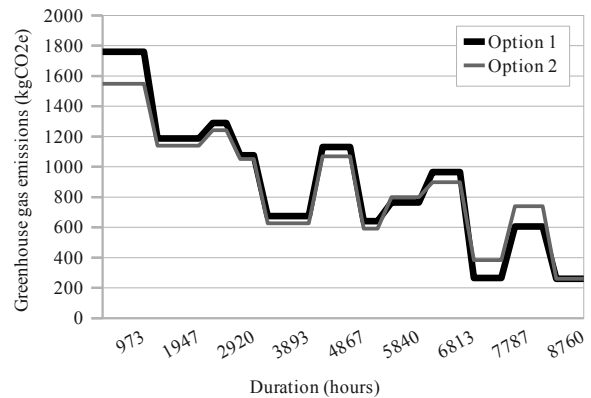


Figure 13: annual greenhouse gas emissions attributed to site (corresponding to heat supply – duration curve).

Note that the emissions curve corresponding to the supply duration curve does not decrease monotonically due to variations in heat supply strategy and the net electrical power imported to or exported from the site. This is illustrated within Fig. 14 and Fig. 15 which show that a significant portion of the annual emissions reduction for option 1 can be attributed to the export of excess power generation from the CHP units. Option 2 on the other hand primarily depends upon the lower embedded emissions of biomass fuel.

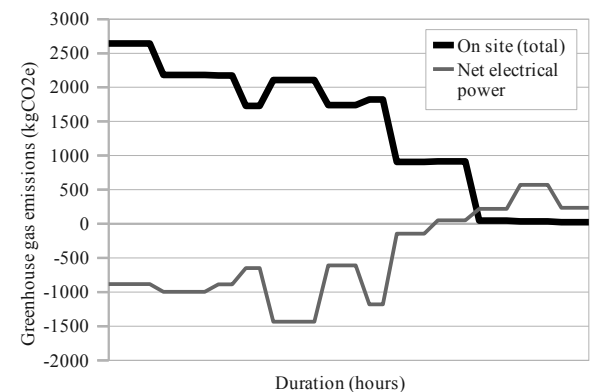


Figure 14: Annual emissions corresponding to the supply-duration curve of option 1.

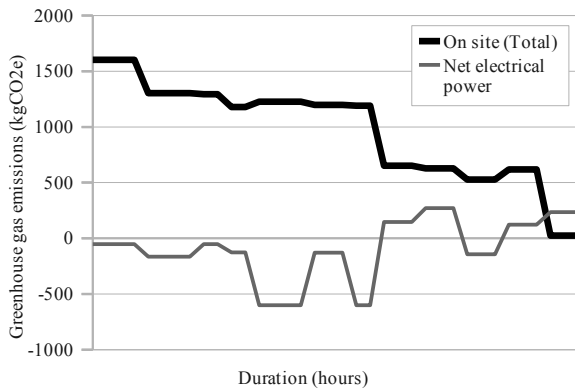


Figure 15: Annual emissions corresponding to the supply-duration curve of option 2.

The similarity with respect to annual emissions savings offers a degree of flexibility within the planning decision process. Option 1, with larger and thus more efficient CHP units, achieves a significantly higher proportion of its emissions savings by exporting electricity to the grid than option 2 and may therefore be a more appropriate solution if local biomass availability is limited. The annual emissions of option 2 on the other hand is more dependent upon the use of biomass and may be preferred if access to local or imported biomass is less restricted.

5 CONCLUSIONS

A modular combined electricity and heat distribution model was developed. The model was applied to study two options integrating biomass community heating with with natural gas CHP. IRR and total annual emissions were determined for each option assuming minimum cost based operation.

Both options delivered significant carbon savings against the individual gas boilers option. Both options were found to deliver an emissions reduction of ~33% when least cost operation was assumed. Option 1 was shown to achieve this primarily through exporting excess electricity to the grid, whilst on site emissions for option 2 were decreased by increasing biomass use.

The benefits of optimally designed integrated infrastructures can be difficult to incorporate into feasibility studies based on conventional analysis methods. This may result in the disregard of potentially cost effective GHG reducing options by inadequate analysis. The combined analysis tool was demonstrated as an effective means of capturing the performance and operational characteristics of integrated multi generation plant distribution networks.

ACKNOWLEDGEMENT

This work was funded by the EPSRC (EP/E04011X/1) via the Supergen Consortium on Future Network Technologies and comprises part of the Supergen Flexnet fu-

ture energy mix work stream. The authors therefore wish to thank the Supergen FlexNet consortium for their continued financial and technical support.

REFERENCES

- [1] Future energy solutions, "Renewable Heat and Heat from combined heat and power plants – study and analysis", published version 1, 2007. <http://webarchive.nationalarchives.gov.uk+/berr.gov.uk/whatwedo/energy/sources/renewables/policy/renewable-heat/page15963.html>
- [2] Carbon trust, "Introducing combined heat and power, a new generation of energy and carbon savings", CTV044, September 2010.
- [3] CHPA, "Integrated energy, the role of CHP and district heating in our energy future", July 2010.
- [4] Earnst and Young, "Renewable Heat Initial Business Case", Report for Defra / BERR, URN 07/1468. September 2007.
- [5] H.M.Government, "Warm Homes, Green Homes ; a strategy for household energy", management supporting paper VII, an enabling framework for district heat and cooling, March 2010.
- [6] S. Kelly and M. Pollit, "An assessment of the present and future opportunities for CHP-DH in the United Kingdom", Energy Policy 38, pp.6936-6945, 2010.
- [7] M. Hinnells, "Combined heat and Power in industry and buildings", Energy Policy 36, pp 4522 – 4526, 2008.
- [8] S. Roberts, "Infrastructure challenges for the built environment", Energy Policy 36, pp. 4563-4567, 2008.
- [9] B. Awad, M. Chaudry, J. Wu and N. Jenkins, "Integrated Optimal Power Flow for Electric Power and Heat in a Microgrid", 20th International Conference on Electricity Distribution, Prague, 8-11 June 2009 .
- [10] J. Soderman and F. Pettersson, "Structural and operational optimisation of distributed energy systems", Applied Thermal Engineering 26, pp.1400-1408, 2006.
- [11] H. Ren, W. Gao, Y. Ruan, "Optimal sizing for residential CHP system", Applied Thermal Engineering 28, pp514-523, 2008.
- [12] M. Geidl and G. Andersson, "Optimal Power Flow of Multiple Energy Carriers", IEEE Transactions of Power Systems, Vol. 22, No. 1, pp. 145-155, February 2007.
- [13] Department of energy and climate change, "Quality assurance for combined heat and power – The CHPQA standard", CHPQA, Issue 3, January 2009.
- [14] W.J. Zhang and X.J. Xie, "DEPSO: Hybrid Particle Swarm with Differential Evolution Operator", IEE International Conference on Systems, Man & Cybernetics (SMCC), Washington D C, USA, pp 3816 – 3821, 2003. <http://www.adaptivebox.net/research/download/index.html>